Biosensors and Bioelectronics 200 (2022) 113921

Contents lists available at ScienceDirect

Biosensors and Bioelectronics

journal homepage: www.elsevier.com/locate/bios

An ultrasensitive biosensor for prostate specific antigen detection in complex serum based on functional signal amplifier and designed peptides with both antifouling and recognizing capabilities

Ni Hui [a,1], Jiasheng Wang [a,1], Dongwei Wang [a], Peipei Wang [c], Xiliang Luo [b,*], Shaoping Lv [c,**]

[a] College of Chemistry and Pharmaceutical Sciences, Qingdao Agricultural University, Qingdao, PR China
[b] Key Laboratory of Sensor Analysis of Tumor Marker, Ministry of Education, College of Chemistry and Molecular Engineering, Qingdao University of Science and Technology, Qingdao, 266042, China
[c] Department of Rehabilitation Medicine, Affiliated Qingdao Central Hospital, Qingdao University, Qingdao, 266042, China

ARTICLE INFO

Keywords:
Antifouling biosensor
Peptide
Electrochemical analysis
Gold nanorod
Prostate specific antigen

ABSTRACT

The development of biosensors capable of averting biofouling and detecting biomarkers in complex biological media remains a challenge. Herein, an ultralow fouling and highly sensitive biosensor based on specifically designed antifouling peptides and a signal amplification strategy was designed for prostate specific antigen (PSA) detection in human serum. A low fouling layer of poly(ethylene glycol) (PEG) doped the conducting polymer poly(3,4-ethylenedioxythiophene) (PEDOT) was electrodeposited on the electrode surface, followed by the immobilization of streptavidin and further attachment of biotin-labelled peptides. The peptide was designed to include PSA specific recognition domain (HSSKLQK) and antifouling domain (PPPPEKEKEKE), and the terminal of the peptide was functionalized with –SH group. DNA functionalized gold nanorods (DNA/AuNRs) were then attached to the electrode, and methylene blue (MB) molecules were adsorbed to the DNA to form the signal amplifier. In the presence of PSA, the peptide was specifically cleaved and resulted in the loss of AuNRs together with DNA and MB, and thus significant decrease of the current signal. The biosensor exhibited a low limit of detection (LOD) of 0.035 pg mL^{-1} (S/N = 3), with a wide linear range from 0.10 pg mL^{-1} to 10.0 ng mL^{-1}, and it was able to detect PSA in real human serum owing to the presence of the antifouling peptides, indicating great potential of the constructed biosensor for practical application.

1. Introduction

Prostate cancer is a major health concern all over the world, and it ranks the 4th place in all the common cancer type (Bolla and Poppel, 2017; Siegel et al., 2018; Szymanski et al., 2010). So far, there is no specific drug for the disease. Therefore, early and accurate detection of tumor biomarkers in body fluids offers a great hope for the treatment of prostate cancer (Mohan et al., 2013). Prostate specific antigen (PSA) is a serine protease (28–32 kDa), which was secreted by normal prostate glandular cells and prostate cancer cells (Zhao et al., 2010). Mature PSA with enzyme activity exists in semen. And some PSA in serum, including PSA-α1-antichymotrypsin, PSA-α2-macroglobulin and free PSA form, has no enzymatic activity (Wu et al., 2004). PSA has been proved to be the most effective and specific serum biomarker for screening prostate cancer, predicting the recurrence after treatment and following up prognosis (Gao et al., 2013; Kingsmore, 2006; Uludag and Tothill, 2012). Numerous traditional methods based on immunoassays have been constructed for the determination of PSA, such as electrogenerated chemiluminescence (Qi et al., 2014a), fluorescence (Taghdisi et al., 2020), surface plasmon resonance (Besselink et al., 2004) and electrochemical method (Dai et al., 2020). These approaches mostly involved the immobilization of PSA antibodies and specific recognition between antigen and antibody (Xie et al., 2015). Thus, immunoassays often suffer from the denaturation of antibody, and the complexity and time-consuming of detection process.

Denmeade et al. reported the action mechanism and kinetic analysis of the short peptide (HSSKLQ) and PSA. The short peptide (HSSKLQ) can be specifically cleaved by PSA (Denmeade et al., 1997) with a high

* Corresponding author.
** Corresponding author.
E-mail addresses: xiliangluo@hotmail.com, xiliangluo@qust.edu.cn (X. Luo), lvshaoping170702@163.com (S. Lv).
[1] These authors contributed equally to this work.

https://doi.org/10.1016/j.bios.2021.113921
Received 16 September 2021; Received in revised form 18 December 2021; Accepted 24 December 2021
Available online 28 December 2021

degree of specificity and good stability in human serum, which was selected as a superior alternative to traditional antibody because of its advantages, such as good stability, low cost and easy to assemble at the molecular level (Iqbal et al., 2000). The K_m (kinetics parameters) for HSSKLQ-AMC is 470 μM. This is 3–5 times that of the previously used PSA matrix, which is mainly chymotrypsin matrix, with a PSA range of 1.3–2 mM (Christensson et al., 1990; Kurkela et al., 1995). Peptide-based electrochemical method has attracted much attention for the detection of PSA for its high sensitivity and convenience. For instance, several electrochemical biosensors based on PSA specific cleavage peptides by employing silver and Au@SiO_2 enhancement or via the host-guest interaction between ferrocene and β-cyclodextrin have been reported (He et al., 2015; Xie et al., 2015). A dual-mode antifouling electrochemical sensing platform for the detection of PSA based on two kinds of antifouling peptides (one of which can be cut by PSA) functionalized with a graphene oxide-Fe_3O_4-thionine probe and internal reference ferrocene, respectively, has also been constructed (Ding et al., 2019). Because the response current signal is small, the sensitivity of the biosensor is barely satisfactory. Therefore, in order to obtain high sensitivity of electrochemical peptide sensors, it is an urgent task to introduce a signal amplification technology into the peptide sensors.

Reasonable use of signal amplifier and improvement of signal output efficiency can effectively improve the sensing performance of electrochemical sensors. Many signal amplification techniques involving nanomaterials, such as metal nanoparticles, carbon quantum dots and graphene oxide, have attracted more and more attention due to their special physical and chemical property (Ahirwal and Mitra, 2010; Du et al., 2010; Jing Qian and Liu, 2010). Amongst them, gold nanomaterials loaded with electroactive reporter molecules have been one of the most commonly used nanomaterials for the signal amplification because of their easy surface modification, synthetic versatility, catalytic property, excellent conductivity and good biocompatibility (Cao et al., 2012; Cui et al., 2015). Methylene blue (MB), the phenothiazine dye, was widely used as electrochemical redox indicators in electrochemical biosensors and MB can interact with single stranded DNA (ssDNA) containing high G/C content or double stranded DNA (dsDNA) based on electrostatic adsorption (Dai et al., 2012; Miao et al., 2016). Therefore, to meet the growing demand for ultrasensitive detection of biomarkers, DNA-modified AuNRs can be designed as signal amplification unit by taking advantage of the strong adsorption capacity of the DNA strands in the composites.

Biosensors face the challenge of serious biofouling in complex environments, especially in real samples. A large number of coexisting protein molecules will be nonspecifically adsorbed on the sensing interface, resulting in biofouling, which can not only block the specific signal, but also greatly reduce the sensitivity and specificity of the biosensors (Jiang et al., 2020). A common way to solve this problem is to integrate the target recognition function into a highly nonfouling surface, thus constructing an antifouling sensing interface. Polyethylene glycol (PEG) and its derivatives possess significant hydrophilic and biocompatible property and have been considered as one of the most widely used antifouling materials. PEG-based antifouling sensing surfaces have been successfully applied to the detection of DNA, microRNA, protein and other disease markers (Dong et al., 2011; Hui et al., 2017). In recent years, zwitterionic peptides composed of natural amino acids can form a hydration layer and have been widely used for the construction of low-fouling biosensors (Walker et al., 2019; Wang et al., 2020b). Jiang's group reported that the zwitterionic peptide (EKEKEKE-PPPPC) showed well-defined secondary structure and outstanding antifouling property in complex media (Nowinski et al., 2012).

In this study, an ultrasensitive and antifouling biosensor was developed for the detection of PSA using PEG doped poly(3,4-ethylenedioxythiophene) (PEDOT) and DNA/AuNRs signal amplifier. PEDOT, as a successful commercial conducting polymer, possesses the well-known excellent properties such as the remarkable conductivity, chemical stability, biocompatibility and well-defined structure (Cui et al., 2016; Mao et al., 2010). A porous antifouling PEG/PEDOT composite was directly electrodeposited onto the surface of a glassy carbon electrode (GCE), which possessed many carboxyl groups, tending to be an ideal substrate for binding multi-functional biomolecules. As shown in Scheme 1, the antifouling peptides were anchored to the PEG/PEDOT through the strong interaction between biotin and streptavidin. The DNA/AuNRs signal amplifier was then attached to the top of the thiol-terminated peptide, followed by the adsorption of Mb onto the DNA/AuNRs. In the presence of PSA, the peptide was specifically cleaved and resulted in the loss of the DNA/AuNRs and MB, and thus the concentration of PSA could be measured through the current signal change of MB. Based on these designed functional materials, an ultrasensitive and antifouling electrochemical biosensor was successfully developed and used for PSA detection in complex media.

2. Experimental

2.1. Materials and apparatus

Hexadecyl trimethyl ammonium bromide (CTAB), chloroauric acid ($HAuClO_4$), sodium borohydride ($NaBH_4$), silver nitrate ($AgNO_3$), ascorbic acid (AA), sodium dodecyl sulfate (SDS), 3,4-Ethylenedioxythiophene (EDOT), $LiClO_4$, MB were purchased from Aladdin regent (Shanghai, China). Streptavidin (SA), N-hydroxysuccinimide (NHS), 1-ethyl-3-(3-dimethylaminopropyl) carbodiimide (EDC), DNA (5′ SH-C6-AGTGCGAGCGAG 3') were purchased from the Sangon Biotech Co., Ltd. (Shanghai, China). Self-designed peptides (Pep1, biotin-PPPPEKEKEKE and Pep2, biotin-PPPPEKEKEKEHSSKLQC) were purchased from Bank-peptide Biological Technology Co. Ltd. (Hefei, China, Fig. S1 and Fig. S2). 4-armed PEG terminated with carboxylic acid groups was purchased from Suzhou Nord Derivatives Pharm-Tech Co., Ltd. Streptavidin, Fetal bovine serum (FBS), human serum albumin (HSA), human hemoglobin (Hg), lysozyme (LYZ), alphafetoprotein (AFP), carcinoembryonic antigen (CEA), human immunoglobulin G (IgG), bovine serum albumin (BSA) and prostate-specific antigen (PSA) were purchased from Beijing Bo Yang Hongda Technology Co., Ltd. (Beijing, China). Human serum samples were provided by the Hospital of Qingdao Agricultural University.

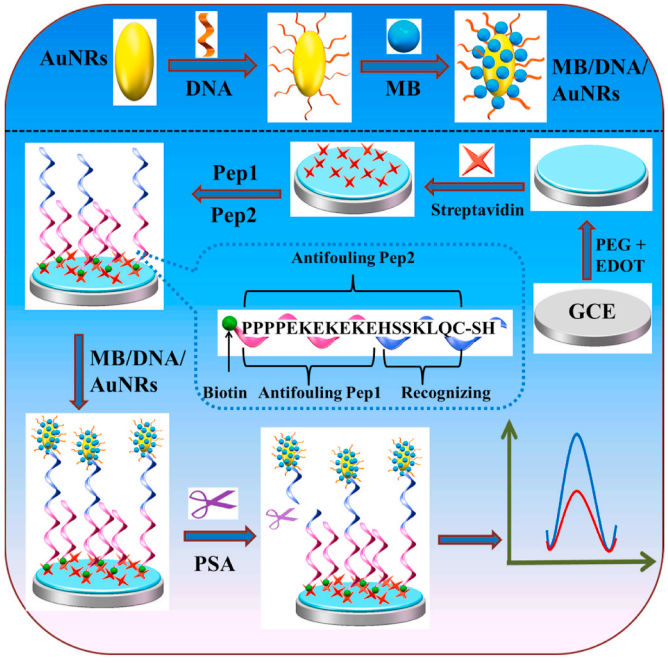

Scheme 1. Schematic diagram and working principle of the antifouling electrochemical biosensor.

For scanning electron microscope (SEM), transmission electron microscopy (TEM), X-Ray photoelectron spectroscopy (XPS), static water contact angle measurements, UV-vis absorbance spectra, confocal laser microscope and all electrochemical experiments, please refer to the instruments in the supporting materials.

2.2. Synthesis of gold nanorods

According to a previous report, AuNRs were prepared using a seed-mediated surfactant-directed approach (Gorelikov and Matsuura, 2008). The preparation method was showed in the supporting materials.

2.3. Synthesis of the DNA/AuNRs signal amplifier

Five groups of the same DNA (10^{-6} mol L^{-1}, 10 μL) were added to five AuNRs solutions (100 μL) with different aspect ratios, respectively, which were incubated at 4 °C for 12 h. To avoid agglomeration, SDS solution (1%, 10 μL) was added into the above solutions and mixed and vibrated at room temperature for 1 h. Then sodium chloride solution (0.5 mol L^{-1}, 50 μL) was added slowly and continued to age for 12 h. After aging, the prepared DNA/AuNRs solutions were washed with PBS solution for three times at 12000 rpm for 20 min, and the collected DNA/AuNRs were dispersed in 1 mL PBS after washing.

2.4. The construction of the electrochemical biosensor

Firstly, the GCEs were polished and cleaned according to the literature (Luo et al., 2010). PEG/PEDOT nanocomposites were electrodeposited onto the GCEs by cyclic voltammetry (CV) technique using 5.0 mL solution containing 10 μL EDOT and 10 mg PEG. The parameters of CV were set as follows: the minimum voltage was - 0.2 V; the maximum voltage was 1.2 V; both the starting and ending voltage were - 0.2 V; the number of deposition cycles was 10 (Fig. S3). The obtained electrode was defined as PEG/PEDOT/GCE. For comparison, $LiClO_4$/-PEDOT/GCE was prepared similarly in 5.0 mL solution containing 10 μL EDOT and 10 mg $LiClO_4$.

The PEG/PEDOT/GCE was incubated in the solution containing streptavidin (10^{-6} mol L^{-1}), NHS (0.1 M) and EDC (0.4 M) for 1 h, and then washed three times with deionized water. The modified electrode was defined as (SA)/PEG/PEDOT/GCE. Then the solution (15 μl, 2.0 mg mL^{-1}) of the two kinds of peptides mixed with the concentration ratio of 1:1 was dropped on the surface of the modified electrode (covered with a moist beaker and lasted for 4 h). The biotin-labelled peptides were immobilized on the electrode surface through the interaction of biotin with streptavidin. The modified electrode was defined as Pep/PEG/PEDOT/GCE.

Five groups of DNA functionalized AuNRs with different aspect ratios were dropped onto five Pep/PEG/PEDOT/GCEs, respectively, and incubated for 10 h to allow the AuNRs to bind to the thiol-terminated peptides by the Au-S bond. After washing, the modified electrodes were immersed in 20 μM MB solutions for 1 h to load the electroactive MB onto the DNA chains, and thus the biosensors (MB/DNA/AuNRs/Pep/PEG/PEDOT/GCEs) were obtained.

All the measurements, such as antifouling assessments, fluorescence imaging and sensing of PSA, were shown in the supporting materials.

3. Results and discussion

3.1. Synthesis and characterization of AuNRs

The AuNRs with various aspect ratios was synthesized by seed-mediated growth method, and five kinds of AuNRs were obtained and characterized. It can be seen from Fig. 1 that sample 1 was almost gold nanoparticles, and the other four samples were AuNRs with different aspect ratios. TEM characterization also showed that AuNRs had good dispersity and uniform shape. Different AuNRs solutions exhibited different colors (Fig. 1A–E), and the UV absorption spectra of the synthesized AuNRs showed that the peak positions of the five kinds of AuNRs are at 540 nm, 660 nm, 702 nm, 748 nm and 831 nm, respectively (Fig. 1F). The concentration of AuNRs in the solution were determined by measuring the absorption peak of AuNRs solution, which was calibrated by inductively coupled plasma atomic emission

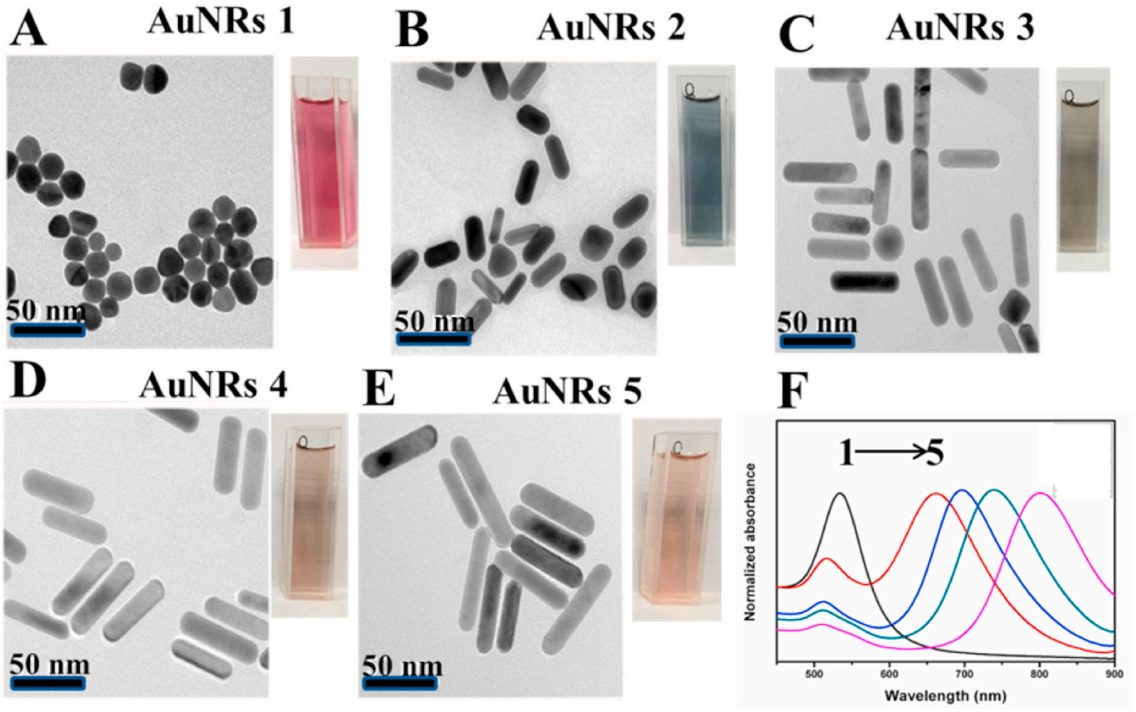

Fig. 1. TEM images and Photograph of AuNRs 1 (A), AuNRs 2 (B), AuNRs 3 (C), AuNRs 4 (D) and AuNRs 5 (E); UV-vis absorbance spectra of AuNRs with different aspect ratios. AuNRs samples 1–5 correspond to A-E.

spectrometry (Orendorff and Murphy, 2015).

3.2. Characterization of the PEG/PEDOT/GCE

The surface morphology and microstructure of the conducting polymers PEDOT doped with $LiClO_4$ and PEG were characterized by SEM. As shown in Fig. 2A, the $LiClO_4$/PEDOT film possessed a relatively flat surface, while the PEG/PEDOT film showed a special three-dimensional porous network microstructure (Fig. 2B–D), which greatly expanded the surface area of the PEG/PEDOT/GCE.

Chronocoulometry technique was used to calculate the electrochemical active surface areas of various electrodes, and the Cottrell formula $[Q(t) = (2nFAD^{1/2}\pi^{-1/2}C)t^{1/2}+Q_{dl} + Q_{ads}]$ (Csiszár et al., 2001) was used. All parameters in the formula are described in related references (Liu et al., 2018; Wang et al., 2020a). On the basis of the experimental results (Fig. S4), the active surface areas of the PEG/PEDOT/GCE (curve c), $LiClO_4$/PEDOT/GCE (curve b) and bare electrode (curve a) was estimated to be 3.03 cm^2, 0.24 cm^2 and 0.033 cm^2, respectively. Interestingly, the active surface area of the PEG/PEDOT/GCE is 91.7 and 12.5 times than that of the bare electrode and $LiClO_4$/PEDOT/GCE, respectively. The PEG/PEDOT/GCE with large electroactive surface area provided a good substrate for the attachment of biomolecules and electron transfer.

3.3. Characterization of the biosensor construction process

The assembly process of PSA biosensor was monitored by CV method step by step. As can be shown from Fig. S5, The redox peak current on the PEG/PEDOT modified electrode (curve b) increased greatly compared with that of the bare electrode (curve a). This large increase in current was due to the excellent conductivity of the conducting polymer PEDOT. The immobilization of peptide on the PEG/PEDOT interface directly led to the reduction of redox peak current (curve c), which was due to the poor electrical conductor of peptide and the electrostatic repulsion between the negative charge of carboxyl group on the peptide and $[Fe(CN)_6]^{3-/4-}$ probes (Wang et al., 2016). After DNA/AuNRs signal amplifiers were assembled onto the modified electrode, the redox peak current at the modified electrode decreased again (curve d), which was due to the repulsion between the negatively charged phosphate skeleton of DNA and the negatively charged electrochemical probes.

Besides, the XPS characterization was chosen as a persuasive way to confirm the construction of the biosensor. As shown in Fig. S6, three elements (O, C and S) were mainly detected in carboxylated PEG derivative doped PEDOT nanocomposites. After the immobilization of streptavidin, N element appeared, which mainly came from the streptavidin (Fig. S6B). After the immobilization of the peptides and the DNA/AuNRs signal amplifiers successively, two new elements (Au and P) appeared (Fig. S6 and Fig. S7), and the Au and P elements were originated from the DNA/AuNRs signal amplifiers. Table S1 showed that the mass contents of Au (0.01%) and P (0.06%) in DNA/AuNRs/PEG/PEDOT (without peptide) were much lower than those of Au (0.07%) and P (1.1%) in DNA/AuNRs/Pep/PEG/PEDOT, proving that the DNA/AuNRs signal amplifier can hardly be fixed onto the sensor without modification with the peptide. These XPS results indicated the preparation of PEG/PEDOT and the subsequent immobilization of the peptides and the signal amplifiers, as well as the successful construction of the biosensor.

3.4. Antifouling performance of various modified interfaces

Nonspecific protein adsorption occurs on the surface contacting with human blood, which will hinder the effectiveness of membranes and biosensors (Qiang et al., 2014). According to Berg's law, among all the possible parameters, water mediated hydrophobic force and hydration forces are considered to be the main factors of protein adsorption. Hydrophilic surface with contact angles less than 65° has the ability to inhibit the nonspecific adsorption of protein, because protein should not be able to replace water from the surface and adsorb (Vogler, 1998). To characterize the surface hydrophilicity and wetting property, the static water contact angles of the bare electrode, $LiClO_4$/PEDOT/GCE,

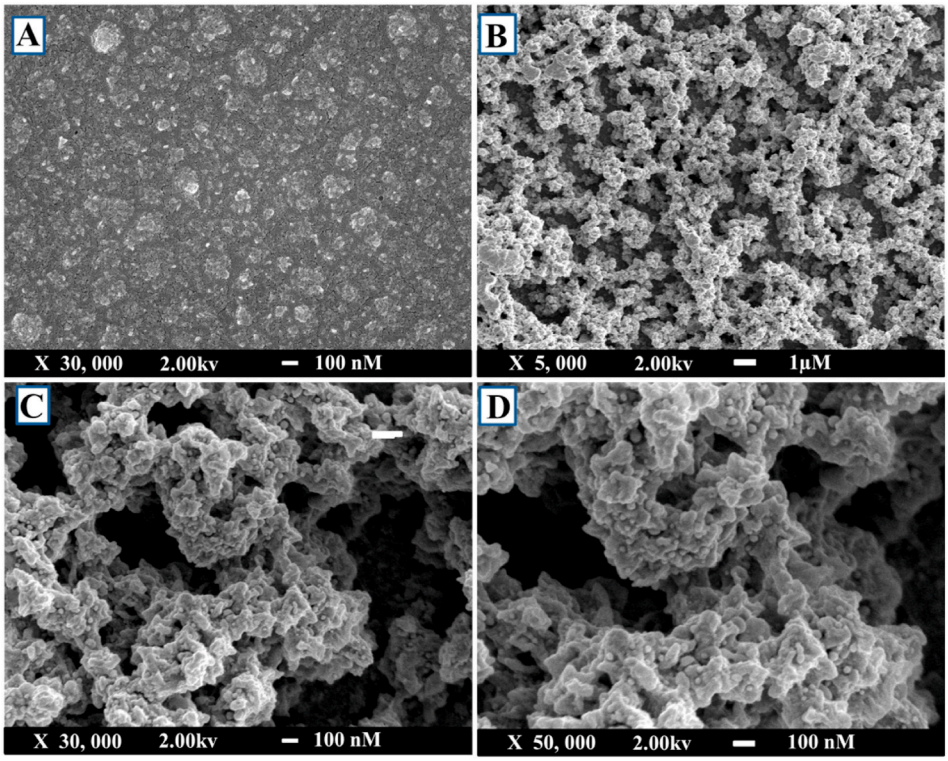

Fig. 2. SEM images of $LiClO_4$/PEDOT (A) and PEG/PEDOT nanocomposites at different magnifications (B–D).

PEG/PEDOT/GCE, SA/PEG/PEDOT/GCE, Pep/PEG/PEDOT/GCE and MB/DNA/AuNRs/Pep/PEG/PEDOT/GCE were tested (Fig. 3B and Table S2). The contact angle of the $LiClO_4$/PEDOT was 40.1°, showing that the synthesized PEDOT film had moderate hydrophilicity. Just as we expected, the contact angles of the PEG/PEDOT/GCE and SA/PEG/PEDOT/GCE greatly decreased to 25.4° and 22.8°, respectively, suggesting strong hydrophilicity of the PEG/PEDOT nanocomposite and SA. After the further modification with peptide and MB/DNA/AuNRs composite, the contact angles of the Pep/PEG/PEDOT/GCE and MB/DNA/AuNRs/Pep/PEG/PEDOT/GCE were reduced to 18.4° and 15.7°, respectively.

To compare the antifouling property of different modified interfaces more intuitively, the bare electrode, $LiClO_4$/PEDOT, PEG/PEDOT, Pep/PEG/PEDOT and MB/DNA/AuNRs/Pep/PEG/PEDOT modified electrodes were incubated in 0.1 mg mL^{-1} FITC-BSA for 1 h. As summarized in Fig. 3A and Fig. S8, the bare electrode and $LiClO_4$/PEDOT modified surface showed the strong fluorescence intensity (serious adsorption of BSA), while the PEG/PEDOT, Pep/PEG/PEDOT and MB/DNA/AuNRs/Pep/PEG/PEDOT modified electrodes showed no significant fluorescence signal (almost no adsorption of BSA).

BSA, HSA, Hg and LYZ were chosen to characterize the antifouling property of the modified electrodes, because these typical proteins have different isoelectric points (pI) and molecular weights. DPV responses of the bare electrode, $LiClO_4$/PEDOT/GCE, PEG/PEDOT/GCE, Pep/PEG/PEDOT/GCE and MB/DNA/AuNRs/Pep/PEG/PEDOT/GCE were compared before and after incubation in different concentration of protein for 30 min (Fig. S9). As shown in Fig. 4, the current change rate ($\Delta I/I_0$) of the bare electrode showed the maximum value, indicating serious adsorption of BSA, HSA, LYZ and Hg on the bare electrode. By contrast, the $\Delta I/I_0$ values of the PEG/PEDOT/GCE, Pep/PEG/PEDOT/GCE and MB/DNA/AuNRs/Pep/PEG/PEDOT/GCE were much smaller than those of the bare electrode and $LiClO_4$/PEDOT/GCE, proving that the PEG/PEDOT, Pep/PEG/PEDOT and MB/DNA/AuNRs/Pep/PEG/PEDOT can greatly reduce the nonspecific protein adsorption.

Complex biological media, such as FBS, were also used to assess the antifouling property of the modified surfaces. As shown in Fig. S10, after immersing in different concentrations of FBS, the oxidation peak currents of the PEG/PEDOT, Pep/PEG/PEDOT and MB/DNA/AuNRs/Pep/PEG/PEDOT modified electrodes changed slightly. More encouragingly, even after incubation in the undiluted FBS, the peak currents of MB/DNA/AuNRs/Pep/PEG/PEDOT/GCE retained 74.02% of their initial value. Due to the good hydrophilicity of the modified surfaces, the PEG/PEDOT, Pep/PEG/PEDOT and DNA/AuNRs/Pep/PEG/PEDOT not only showed the antifouling ability to single protein, but also showed excellent antifouling ability to complex biological samples.

3.5. *Electrochemical detection of PSA with the biosensor*

To confirm the feasibility of the biosensor, MB redox indicator adsorbed in signal amplifiers was used to enhance the sensitive signal in PSA detection using the change of DPV signals before and after PSA incubation. Fig. S11 showed that the biosensor exhibited well-defined

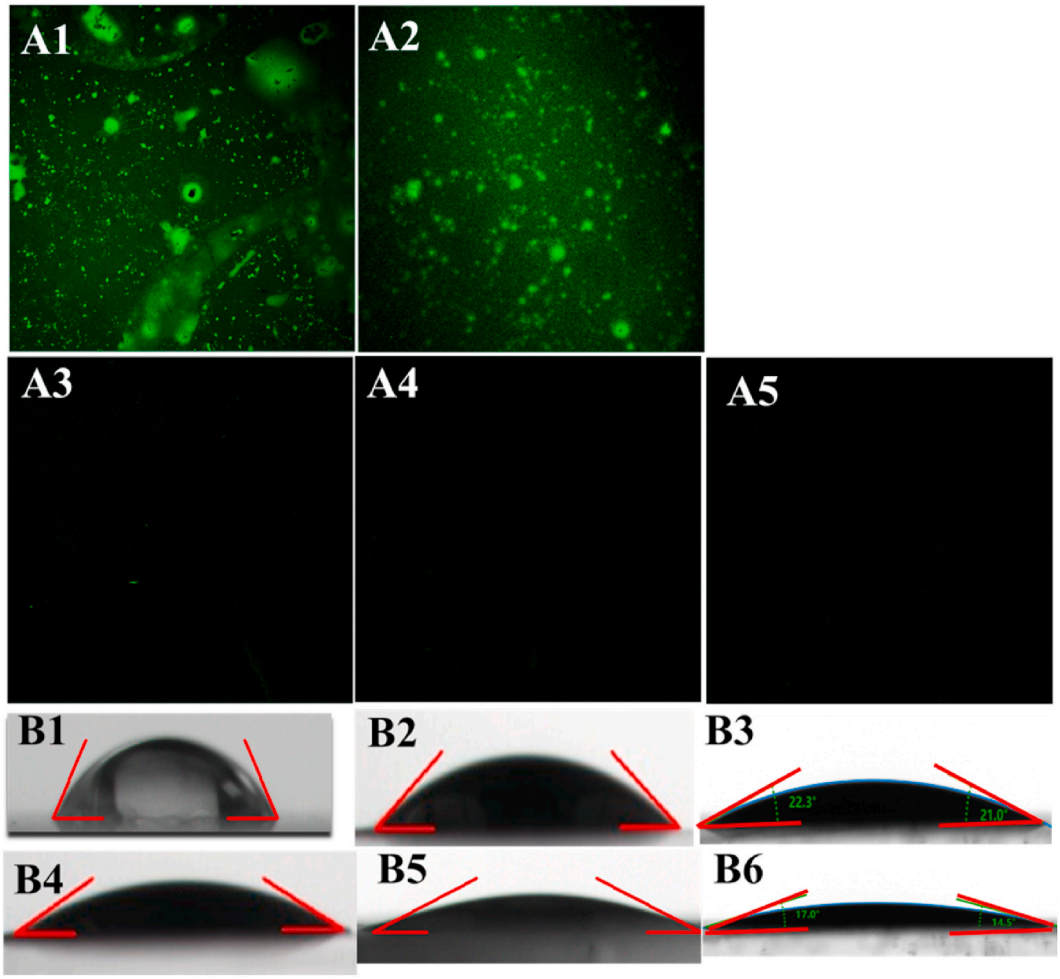

Fig. 3. Fluorescence microscopy images of the bare electrode (A1), $LiClO_4$/PEDOT (A2), PEG/PEDOT (A3), Pep/PEG/PEDOT (A4) and MB/DNA/AuNRs/Pep/PEG/PEDOT (A5) modified electrodes. The contact angle images of the bare electrode (B1), $LiClO_4$/PEDOT (B2), PEG/PEDOT (B3), (SA)/PEG/PEDOT/GCE (B4), Pep/PEG/PEDOT/GCE (B5), and MB/DNA/AuNRs/Pep/PEG/PEDOT/GCE (B6).

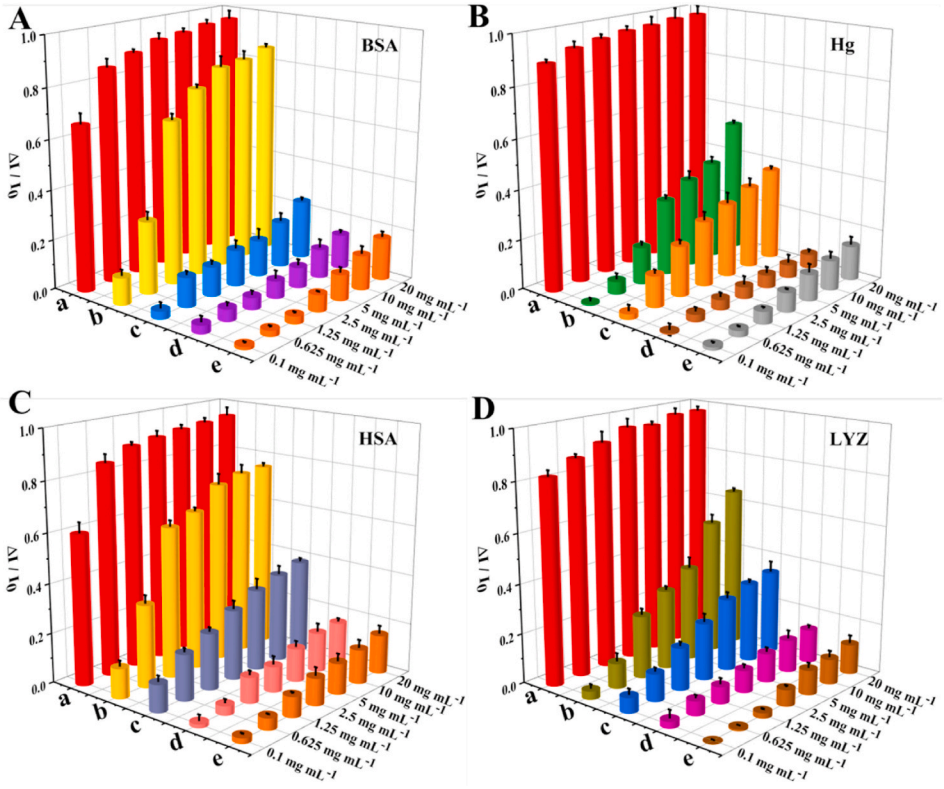

Fig. 4. Antifouling performance of four kinds of modified electrodes against different concentration of protein (a: the bare electrode, b: $LiClO_4$/PEDOT/GCE, c: PEG/PEDOT/GCE, d: Pep/PEG/PEDOT/GCE and e: MB/DNA/AuNRs/Pep/PEG/PEDOT/GCE). Error bars represented the standard deviations across three repeated measurements (n = 3).

DPV signals, which corresponds to the electrochemical oxidation of MB (Li et al., 2015). After incubation in PSA, the electrochemical current signal of the biosensor decreased significantly, indicating that the MB remained on the biosensor was reduced by PSA specific cleavage of peptide. Therefore, the PSA detection was performed based on measuring the electrochemical signal change of the MB oxidation peak.

To obtain optimal conditions for PSA assay, the effects of the PEG/PEDOT deposition mass, the aspect ratios of AuNRs, and PSA incubation

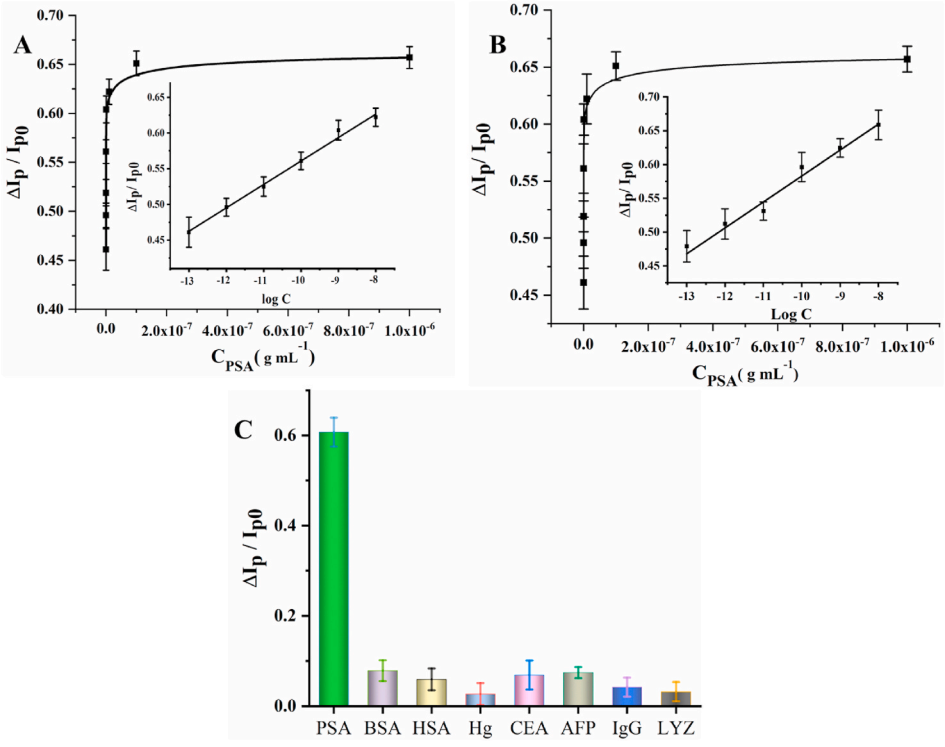

Fig. 5. Current change rate ($\Delta I_p/I_{p0}$) of the biosensor for PSA in PBS 7.4 (A) and in 5% FBS (B). Insets show the linear relationships between the signal change rate ($\Delta I_p/I_{p0}$) and the logarithm of the concentration. (C) The response of the biosensor towards PSA and BSA, HSA, Hg, CEA, AFP, IgG and LYZ. The concentration of PSA was 1.0 ng mL^{-1}, and the concentration of other proteins was 10.0 ng mL^{-1}. Error bars represented the standard deviations across three repeated measurements (n = 3).

time on the signal change rate ($\Delta I_p/I_{p0}$) were investigated in detail, as shown in Fig. S12. Based on the experimental results, the following experimental conditions were adopted. (A) CV cycles of PEG/PEDOT electrodeposition was 15 cycles; (B) the aspect ratios of AuNRs was sample 2; (C) the PSA incubation time was 30 min.

The response of the antifouling biosensor to various amounts of PSA was investigated by the sensitive DPV method. As shown in Fig. S11, the PSA biosensor demonstrated an excellent association with different amount of PSA in the optimized condition. As expected, along with the increase of the PSA concentration, the electrochemical response of the engineered PSA biosensor decreased dramatically along with the increase of the PSA concentration, due to the enhanced cleavage of the signal amplifier by PSA. A linear relationship was obtained between the signal change rate ($\Delta I_p/I_{p0}$) and the logarithm of the PSA concentrations ranging from 0.10 pg mL^{-1} to 10.0 ng mL^{-1} (Fig. 5A). The regression equation was $\Delta I_p/I_{p0} = 0.0328 \log C + 0.889$ ($R^2 = 0.99$). The limit of detection (LOD) was estimated to be 0.035 pg mL^{-1} (S/N = 3), which was far lower than the reported value in Table S3 (Chen et al., 2014; Ding et al., 2019; Hun et al., 2015; Qi et al., 2014b; Xie et al., 2015). In addition, different concentrations of PSA in 5% FBS was assayed by the proposed biosensor. As shown in Fig. 5B, the linear regression equation was $\Delta I_p/I_{p0} = 0.0384 \log C + 0.967$ ($R^2 = 0.98$), which was similar to the calibration curves obtained in PBS. This indicated that the biosensor had a high possibility of practical application in complex samples. This high analytical performance of the biosensor are mainly contributed to the nanoporous microstructure and antifouling property of the PEG/-PEDOT, powerful signal amplification function of DNA/AuNRs signal amplifiers and the specific strong cleavage by the target PSA.

3.6. Specificity, reproducibility and stability of the PSA biosensor

The selectivity of the PSA biosensor was verified with possible interfering proteins, such as PSA, BSA, HSA, Hg, LYZ, IgG, AFP and CEA. As shown in Fig. 5C, a remarkable decrease in signal change rate is observed for PSA (1.0 ng mL^{-1}), while negligible responses are found for other proteins (10.0 ng mL^{-1}). Therefore, the prepared PSA biosensor was not affected by various interfering proteins, indicating good specificity of the biosensor.

The long-term stability of DNA/AuNRs and the PSA biosensor was also investigated. The newly prepared DNA/AuNRs were stored at 4 °C in PBS, and DNA/AuNRs stored for different time periods were used to modify the electrodes, and the prepared biosensor responses were recorded. As shown in Fig. S13 A, the biosensor responses did not change significantly, indicating excellent long-term stability of the DNA/AuNRs. The storage stability of the biosensors was evaluated by measuring the responses of a batch of biosensors stored for different days (three new biosensors were used for the measurement at each time period). The responses of biosensors stored for one week were similar to those of the newly prepared biosensors, but the responses of biosensors stored for longer time gradually decreased. The intra- and inter-assays was performed to evaluate the reproducibility of this method. When five biosensors were used to test the same concentration of PSA (1.0 ng mL^{-1}), the relative standard deviation (RSD) of biosensors was 5.1% (Fig. S13B). When the same electrode was used to repeat the detection for five times at a certain concentration of PSA (1.0 ng mL^{-1}), The RSD of five results was 5.2% (Fig. S13C).

3.7. Analytical application in real samples

To evaluate the accuracy of the biosensor, it was also implemented in determining the PSA concentrations in the undiluted real human serum samples, and the standard addition method was used. As shown in Table S4, the detection recoveries were in the range of 101.6%–107.0% and the RSD values from 3.2% to 6.1%, which are acceptable for real sample analysis. The results indicated that the biosensor has a promising potential for practical detection of PSA in serum samples.

4. Conclusion

In summary, an antifouling and ultrasensitive PSA biosensor capable of detecting targets in human serum was constructed based on the antifouling and PSA specific cleavage peptides, and the DNA/AuNRs signal amplifier. Three factors herein ensured the unique and excellent sensing performance of the biosensor: Firstly, the designed peptides including antifouling zwitterionic domain and PSA-induced cleavage domain provided good selectivity and antifouling ability of the biosensor in complex biological environment. Secondly, the signal amplifier system of the DNA/AuNRs and MB ensured high sensitivity of the electrochemical biosensor. Thirdly, the PEG/PEDOT provided a three-dimensional porous substrate with large electroactive surface area, excellent electrical conductivity and antifouling capability. The proposed strategy for the development of electrochemical biosensors with ultrahigh sensitivity and ultralow fouling based on the PEG/PEDOT platform associated with DNA/AuNRs signal amplifier and designed peptides offered an effective way for the construction of various biosensors and bioelectronics for assaying targets in complex biological media.

CRediT authorship contribution statement

Ni Hui: Conceptualization, Methodology, Investigation, Writing – original draft, Visualization, Data curation. **Jiasheng Wang:** Conceptualization, Investigation, Data curation, Writing – review & editing. **Dongwei Wang:** Resources, Data curation, Writing – review & editing. **Peipei Wang:** Resources, Methodology, Writing – review & editing. **Xiliang Luo:** Conceptualization, Methodology, Writing – review & editing, Visualization, Supervision. **Shaoping Lv:** Conceptualization, Resources, Visualization, Funding acquisition.

Declaration of competing interest

The authors declare that they have no known competing financial interests or personal relationships that could have appeared to influence the work reported in this paper.

Acknowledgments

This work was funded by the National Natural Science Foundation of China (21705088), the National Key Technology R&D Program of China (2017YFD0501500), the Shandong Provincial Peanut Industry Technology System Project (SDAIT-04-09), and the pharmaceutical scientific research guidance plan of Qingdao (2020-WJZD079, 2020-WJZD073).

Appendix A. Supplementary data

Supplementary data to this article can be found online at https://doi.org/10.1016/j.bios.2021.113921.

References

Ahirwal, G.K., Mitra, C.K., 2010. Biosens. Bioelectron. 25 (9), 2016–2020.
Besselink, G., Kooyman, R., Os, P., Engbers, G., Schasfoort, R., 2004. Anal. Biochem. 333 (1), 165–173.
Bolla, M., Poppel, H.V., 2017. Springer Chapter 1, 1–27.
Cao, Y., Yuan, R., Chai, Y., Mao, L., Niu, H., Liu, H., Ying, Z., 2012. Biosens. Bioelectron. 31 (1), 305–309.
Chen, X., Zhou, G., Song, P., Wang, J., Gao, J., Lu, J., Fan, C., Zuo, X., 2014. Anal. Chem. 86 (15), 7337–7342.
Christensson, A., Laurell, C.B., Hans, L., 1990. Eur. J. Biochem. 194, 755–765.
Csiszar, M., Szucs, A., Tolgyesi, M., Mechler, A., Novak, M., 2001. J. Electroanal. Chem. 497 (1), 69–74.
Cui, H.F., Xu, T.B., Sun, Y.L., Zhou, A.W., Cui, Y.H., Liu, W., Luong, J., 2015. Anal. Chem. 87 (2), 1358–1365.
Cui, M., Wu, Y., Fan, X., Song, Z., Luo, X., Guo, B., 2016. Biosens. Bioelectron. 79, 736–741.
Dai, Y., Wang, X., Zhu, X., Liu, H., Luo, C., 2020. Microchim. Acta 187 (8), 428.
Dai, Z., Hu, X., Wu, H., Zou, X., 2012. Chem. Commun. 48 (12), 1769–1771.

Denmeade, S.R., Lou, W., Lövgren, J., Malm, J., Isaacs, J.T., 1997. Cancer Res. 57 (21), 4924.
Ding, C., Wang, X., Luo, X., 2019. Anal. Chem. 91, 15846–15852.
Dong, B., Manolache, S., Wong, A., Denes, F.S., 2011. Polym. Bull. 66 (4), 517–528.
Du, D., Zou, Z., Shin, Y., Wang, J., Wu, H., Engelhard, M.H., Liu, J., Aksay, I.A., Y, L., 2010. Anal. Chem. 82 (7), 2989–2995.
Gao, Z., Xu, M., Hou, L., Chen, G., Tang, D., 2013. Anal. Chem. 85 (14), 6945–6952.
Gorelikov, I., Matsuura, N., 2008. Nano Lett. 8 (1), 369–373.
He, Y., Xie, S., Yang, X., Yuan, R., Chai, Y., 2015. ACS Appl. Mater. Interfaces 7 (24), 13360–13366.
Hui, N., Sun, X., Niu, S., Luo, X., 2017. ACS Appl. Mater. Interfaces 9 (3), 2914–2923.
Hun, X., Xu, Y., Luo, X., 2015. Microchim. Acta 182 (9–10), 1669–1675.
Iqbal, S.S., Mayo, M.W., Bruno, J.G., Bronk, B.V., Chambers, J.P., 2000. Biosens. Bioelectron. 15 (11–12), 549–578.
Jiang, C., Wang, G., Hein, R., Liu, N., Luo, X., Davis, J.J., 2020. Chem. Rev. 120 (8), 3852–3889.
Jing Qian, C.Z., Cao, Xiaodong, Liu, S., 2010. Anal. Chem. 82 (15), 6422–6429.
Kingsmore, S.F., 2006. Nat. Rev. Drug Discov. 5 (4), 310–320.
Kurkela, R., Herrala, A., Henttu, P., Nal, H., Vihko, P., 1995. Biotechnology 13 (11), 1230–1234.
Li, F., Peng, J., Zheng, Q., Guo, X., Tang, H., Yao, S., 2015. Anal. Chem. 87 (9), 4806–4813.
Liu, S., Ma, Y., Cui, M., Luo, X., 2018. Sensor. Actuator. B. 255 (Pt.3), 2568–2574.
Luo, X., Killard, A.J., Smyth, M.R., 2010. Chem. Eur J. 13 (7), 2138–2143.
Mao, H., Liu, X., hao, D.C., Cui, L., Li, Y., Zhang, W., Wang, C., 2010. J. Mater. Chem. 20 (45), 10277–10284.
Miao, Xiangmin, Zongbing, Zhu, Aihua, Feng, Zhaozhong, Tian, Jun, Peng, 2016. Biosens. Bioelectron. 83, 39–44.
Mohan, K., Donavan, K.C., Arter, J.A., Penner, R.M., Weiss, G.A., 2013. J. Am. Chem. Soc. 135 (20), 7761–7767.
Nowinski, A.K., Fang, S., White, A.D., Keefe, A.J., Jiang, S., 2012. J. Am. Chem. Soc. 134 (13), 6000–6005.
Orendorff, C.J., Murphy, C.J., 2015. J. Phys. Chem. B 110 (9), 3990–3994.
Qi, H., Li, M., Dong, M., Ruan, S., Gao, Q., Zhang, C., 2014a. Anal. Chem. 86 (3), 1372–1379.
Qi, H., Li, M., Dong, M., Ruan, S., Gao, Q., Zhang, C., 2014b. Anal. Chem. 86, 1372–1379.
Wei, Qiang, Becherer, Tobias, Angioletti-Uberti, Stefano, Joachim, Dzubiella, Christian, Wischke, 2014. Angew. Chem. Int. Ed. 53 (31), 8004–8031.
Siegel, R.L., Miller, K.D., Jemal, A., 2018. CA A Cancer J. Clin. 68 (1), 7–30.
Szymanski, K.M., Wheeler, D.C., Mucci, L.A., 2010. Am. J. Clin. Nutr. 92 (5), 1223.
Taghdisi, S.M., Danesh, N.M., Nameghi, M.A., Ramezani, M., Abnous, K., 2020. Anal. Chim. Acta 1120, 36–42.
Uludag, Y., Tothill, I.E., 2012. Anal. Chem. 84 (14), 5898–5904.
Vogler, E.A., 1998. Adv. Colloid Interface Sci. 74, 69–117.
Walker, J.A., Robinson, K.J., Munro, C., Gengenbach, T., Muller, D.A., Young, P.R., Lua, L.H.L., Corrie, S.R., 2019. Langmuir 35 (5), 1266–1272.
Wang, G., Han, R., Su, X., Li, Y., Xu, G., Luo, X., 2016. Biosens. Bioelectron. 92, 396–401.
Wang, H., Lü, H., Yang, L., Song, Z., Hui, N., 2020a. Anal. Chim. Acta 1139, 155–163.
Wang, J., Wang, D., Hui, N., 2020b. Bioelectrochemistry 136, 107595.
Wu, P., Lei, Z., Stenman, U.H., Leinonen, J., 2004. Clin. Chem. 50, 125–129.
Xie, S., Zhang, J., Yuan, Y., Chai, Y., Yuan, R., 2015. Chem. Commun. 51 (16), 3387–3390.
Zhao, N., He, Y., Mao, X., Sun, Y., Zhang, X., Li, C., Lin, Y., Liu, G., 2010. Electrochem. Commun. 12, 471–474.